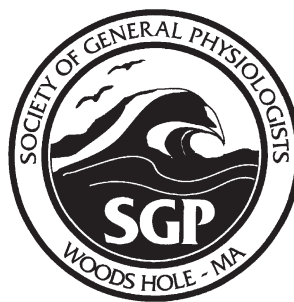


Abstracts of Papers at The Sixty-Third  
Annual Meeting of The Society  
of General Physiologists

# MUSCLE in Health and Disease

Marine Biological Laboratory  
Woods Hole, Massachusetts  
9–13 September 2009



Organized by  
DAVID EISNER and H. LEE SWEENEY

## SESSION I: THE MOTOR

### 1. Effect of Levosimendan on Slow Force Response to Sudden Stretch in Isolated Rat Papillary Muscle. OLEG LOOKIN, R. LISIN, and YURI LEONIDOVICH PROTSENKO, *Institute of Immunology and Physiology of Russian Academy of Science, Ekaterinburg 620219, Russia*

We tested whether change of Ca sensitivity of TnC is involved to slow force response (SFR) in health cardiac muscle. For that, we used levosimendan (LS). Rat RV papillary muscles were suddenly stretched from 85 to 95% of  $L_{MAX}$ , and force and calcium transient were measured during SFR in control solution and at 0.1, 1, and 10  $\mu\text{M}$  LS. Muscles were washed in Krebs (25°C, 0.33 Hz) with 1.1 and 2.5 mM  $[\text{Ca}^{2+}]_o$  to evaluate the effect of calcium sensitization on SFR at different Ca-saturation levels.

LS decreased twitch force on any stage of SFR, but more pronouncedly at pre-stretch length and in lesser degree immediately after stretch. Regardless of  $[\text{Ca}^{2+}]_o$  and stage of SFR, LS significantly and dose dependently decreased time-to-peak tension and accelerated twitch relaxation, with no effect to peak  $[\text{Ca}^{2+}]_i$ . Nevertheless, LS dose dependently increased  $T_{80}$  and decreased  $T_{20}$  of Ca transient relaxation.

Regardless of  $[\text{Ca}^{2+}]_o$  concentration, SFR was either biphasic (fast initial rise, slow fall until steady state) or triphasic (fast initial rise, slow fall, slow rise). Some preparations showed apparent LS dose-dependent increase of total SFR, whereas others showed the opposite effect. We have fitted fast initial rise of SFR by the equation  $F(t) = A*(1 - e^{Bt})$ . At all LS, the A parameter (amplitude) was significantly increased to  $\sim 130\%$  relatively control, whereas the B parameter (time constant) was lower than in control (not significantly). The effect was not dependent on  $[\text{Ca}^{2+}]_o$ .

Therefore, fast force response to sudden stretch (during  $\sim 30$  s) in rat myocardium might be at least partially due to changed Ca sensitivity of TnC to  $\text{Ca}^{2+}$ . Slow response (several minutes after stretch) is caused by slow dynamics of intracellular  $\text{Ca}^{2+}$  rather than further change in Ca sensitivity. It is also possible that in the range of 0.1 to 10  $\mu\text{M}$ , LS acts not only as a calcium sensitizer, but it also increases cAMP levels, which could explain accelerated relaxation.

### 2. Dystrophin and Utrophin Have Distinct Effects on the Microsecond Dynamics of Actin. EWA PROCHNIEWICZ, DAVIN HENDERSON, AVA YUN LIN, JAMES ERVASTI, and DAVID D. THOMAS, *Department of Biochemistry, Molecular Biology and Biophysics, University of Minnesota, Minneapolis, MN 55455*

Dystrophin and utrophin bind actin in vitro with similar affinities, but with different molecular contacts. These differences are proposed to alter the elasticity of actin-dystrophin and actin-utrophin linkages to the sarcolemma, affecting the cell's response to muscle stretches. To test this hypothesis, we have determined the effects of dystrophin and utrophin on the microsecond dynamics of erythrosin iodoacetamide-labeled actin using transient phosphorescence anisotropy (TPA). Binding of dystrophin or utrophin to actin resulted in significant changes in the TPA decay. At a low level of actin saturation ( $\leq 20\%$ ), both proteins induced similar changes in actin dynamics, but at higher levels of saturation, utrophin was more effective than dystrophin and induced more pronounced changes in the final anisotropy, correlation time, and initial anisotropy of actin. The simplest interpretation of these changes is that utrophin restricted the amplitude and increased the rates of motion of the probe to a substantially larger extent than dystrophin. Further analysis indicated that the actin-utrophin complex is much more torsionally flexible than the actin-dystrophin complex. In addition, individual regions along the full-length proteins have unique properties that contribute differently to the effects on actin dynamics. Preliminary data on fragments containing all the proposed actin binding domains (DN-R17/UN-R10) show less effect on regulating rotational amplitude and nearly no effect on rotational rate. Future experiments will investigate other fragments of dystrophin and utrophin and their functionally relevant mutants to determine which structural elements of these proteins are critical in determining the flexibility of actin filaments, and what level of actin flexibility is physiologically optimal. In addition, site-directed labeling of dystrophin and utrophin will permit spectroscopic analysis of these proteins' structural dynamics when free and bound to actin. These results will greatly aid in both understanding the pathophysiology of DMD and optimizing therapeutic designs using micro-dystrophin/micro-utrophin or antisense oligonucleotides.

### 3. Assessment of the Effect of Cardiac Myosin Binding Protein C on "pCa-Velocity" Relationship Obtained in an In Vitro Motility Assay. D.V. SHCHEPKIN, G.V. KOPYLOVA, B.Y. BERSHITSKY, and L.V. NIKITINA, *Institute of Immunology and Physiology of the Russian Academy of Science, Yekaterinburg 620219, Russia*

An in vitro motility assay with regulated thin filaments was applied to assess a modulatory role of cardiac myosin binding protein C (cMyBP-C) on myosin motion regulation. A series of experiments was performed to obtain dependences of thin filament movement velocity on calcium concentration in solution (in the range

of  $pCa = 5$  to  $pCa = 8$ ). Rabbit cardiac myosin with and without rabbit cMyBP-C was used. Corresponding “ $pCa$ –velocity” curves revealed sigmoid form.

Insertion of cMyBP-C to the motility assay affected distinctly thin filament sliding velocities at maximal calcium levels. Particularly, adding 130 nM cMyBP-C resulted in a 43% slowing of thin filament speed at saturating calcium concentration ( $pCa = 5$ ) as compared with regulated thin filaments without cMyBP-C ( $2.08 \pm 0.12 \mu\text{m/s}$  vs.  $3.65 \pm 0.04 \mu\text{m/s}$ , respectively). The presence of cMyBP-C did not change calcium sensitivity estimated as  $pCa_{50}$  ( $pCa$  value corresponding to half maximum velocity). Hill coefficients of cooperativity ( $h$ ) were determined for  $pCa$ –velocity relationships. The value of  $h$  did not differ significantly due to the cMyBP-C addition and varied around 6.

Our data found in the experiments with cardiac myosin are in good agreement with the results obtained with skeletal myosin by others (Saber, W., K.J. Begin, D.M. Warshaw, and P. VanBuren. 2008. *J. Mol. Cell. Cardiol.* 44:1053–1061; Razumova, M.V., J.F. Shaffer, A.Y. Tu, G.V. Flint, M. Regnier, and S.P. Harris. 2006. *J. Biol. Chem.* 281:35846–35854). Thus, the addition of cMyBP-C to the motility assay using both cardiac and skeletal myosin resulted in the slowing of thin filament velocity at a saturating calcium concentration. However, our experimental model seems to be more relevant to the acto–myosin interaction in intact cardiomyocytes.

This work was supported by Program 27 of Presidium RAS.

#### 4. Insights into Myosin Function Based on the Kinetic and Structural Data. **H. LEE SWEENEY**, *University of Pennsylvania School of Medicine, Philadelphia, PA 19104*

The sliding of actin and myosin filaments was proposed as the basis of force generation and shortening in striated muscle. Although this is now generally accepted, the detailed molecular mechanism of how myosin uses ATP to generate force during its cyclic interaction with actin is only now being unraveled. New insights have come from the unconventional myosins, especially myosin V and, more recently, myosin VI. These myosins are kinetically tuned to allow movement on actin filaments as a single, dimeric molecule, which has led to new kinetic, mechanical, and structural data that have filled in missing pieces of the actomyosin–chemo–mechanical transduction puzzle.

#### 5. The Actomyosin Motor: Structure, Function, and Modulation, One Molecule at a Time. **DAVID M. WARSHAW**, *University of Vermont College of Medicine, Burlington, VT, 05405*

Myosin is a double-headed molecular motor that cyclically interacts with actin to generate force and motion with the energy derived from its hydrolysis of ATP. Using a combination of single molecule biophysical

techniques and structural mutagenesis, critical domains of the myosin motor have been identified that are essential for force and motion generation as well as effective communication between its two heads. With this knowledge, the molecular consequences of point mutations in both myosin and actin that lead to genetic forms of human cardiomyopathies can be understood.

## SESSION II: ORGANIZATION, REGULATION, AND DISEASES OF THE CONTRACTILE APPARATUS

#### 6. During Muscle Atrophy, Components of the Thick, But Not Thin, Filaments Are Degraded by MuRF1-dependent Ubiquitylation. **SHENHAV COHEN, JEFFREY J. BRAULT, STEVEN P. GYGI, DAVID J. GLASS, DAVID M. VALENZUELA, CARLOS GARTNER, ESTHER LATRES, and ALFRED L. GOLDBERG**, *Department of Cell Biology, Harvard Medical School, Boston, MA 02115*

Loss of myofibrillar proteins is a hallmark of atrophying muscle. Expression of MuRF1, a ubiquitin ligase, is markedly induced during atrophy, and MuRF1 deletion attenuates muscle wasting. We generated mice expressing a Ring-deletion mutant MuRF1, which binds but cannot ubiquitylate substrates. Mass spectrometry of the bound proteins in denervated muscle identified many myofibrillar components. Upon denervation or fasting, atrophying muscles show a loss of myosin binding protein C (MyBP-C) and myosin light chains 1 and 2 (MyLC1 and MyLC2) from the myofibril before any measurable decrease in myosin heavy chain (MyHC). Their selective loss requires MuRF1. MyHC is protected from ubiquitylation in myofibrils by associated proteins, but it eventually undergoes MuRF1-dependent degradation. In contrast, MuRF1 ubiquitylates MyBP-C, MyLC1, and MyLC2, even in myofibrils. Because these proteins stabilize the thick filament, their selective ubiquitylation may facilitate thick filament disassembly. However, the thin filament components decreased by a mechanism not requiring MuRF1.

#### 7. The Mechanical Properties of Titin Molecules Isolated from the Failing Heart. **HELEN K. GRAHAM, MICHAEL J. SHERRATT, and ANDREW W. TRAFFORD**, *School of Medicine, University of Manchester, Manchester M13 9PT, England, UK*

The passive stiffness of cardiac muscle is primarily determined by the giant protein titin. Alterations in the ratio of the relatively stiff (N2B) to compliant (NB2BA) titin isoforms have been identified in both coronary artery disease and non-ischemic dilated cardiomyopathy in the presence of decreased titin-based passive stiffness (Makarenko, I., C.A. Opitz, M.C. Leake, C. Neagoe, M. Kulke, J.K. Gwathmey, F. del Monte, R.J. Hajjar, and W.A. Linke. 2004. *Circ. Res.* 95:708–716; Neagoe, C., M.

Kulke, F. del Monte, J.K. Gwathmey, P.P. de Tombe, R.J. Hajjar, and W.A. Linke. 2002. *Circulation*. 106:1333–1341). It has been proposed, therefore, that changes in the mechanical properties of titin play a major role in the etiology of heart disease. This study aimed to determine if the tensile strength of isolated titin molecules is altered in the failing heart.

Heart failure was induced in adult male ferrets by ascending aortic coarctation (Graham, H.K., and A.W. Trafford. 2007. *Am. J. Physiol.* 292:H1364–H1372). All procedures accorded with The UK Animals (Scientific Procedures) Act, 1986. Titin molecules were isolated from the left ventricle (Soteriou, A., M. Gamage, and J. Trinick. 1993. *J. Cell Sci.* 104:119–123) and aligned and stretched by a molecular combing technique that uses a receding meniscus to apply a tensile force of  $\sim 60$  pN (Tskhovrebova, L., and J. Trinick. 1997. *J. Mol. Biol.* 265:100–106; Sherratt, M.J., C. Baldock, J.L. Haston, D.F. Holmes, C.J. Jones, C.A. Shuttleworth, T.J. Wess, and C.M. Kiely. 2003. *J. Mol. Biol.* 332:183–193).

After molecular combing, titin molecules were visualized by atomic force microscopy. In contrast to non-combed molecules, combed titin appeared straightened and beaded with discernable filaments between beads. The mean molecular diameter of titin (calculated as height above substrate) was decreased in failing hearts compared with control ( $0.26 \pm 0.001$  vs.  $0.33 \pm 0.001$  nm;  $P < 0.001$ ;  $n = 104$ –130 molecules, 3 animals per group). This difference was more pronounced in the shorter molecules ( $<3.5$   $\mu$ m).

The mean distance between beads was increased in failing hearts ( $49.3 \pm 1.5$  vs.  $126.8 \pm 4.5$  nm;  $P < 0.001$ ;  $n = 370$ –429, 3 animals per group). No significant difference was observed in the mean contour lengths of titin from sham and heart failure tissue after molecular combing.

In conclusion, the decreased titin molecular diameter combined with an increased inter-bead distance suggests that titin from failing hearts is less resistant to tensile forces when compared with control, and it may help to explain the decreased titin-based passive tension observed in diseased hearts.

#### 8. Myosin Binding Protein C Function in Cardiac Muscle. **SAMANTHA P. HARRIS, JUSTIN F. SCHAFFER, and KRISTINA L. BEZOLD, University of California, Davis, Davis, CA 95618**

Myosin binding protein C (MyBP-C) is a thick filament protein of vertebrate sarcomeres that limits cross-bridge cycling kinetics and reduces myocyte power output. Mutations in the gene encoding cardiac MyBP-C are a leading cause of inherited cardiomyopathies, but the mechanisms by which MyBP-C affects cardiac function and by which mutations in cMyBP-C cause disease are not well understood. Here, we investigated the ability of the first four N-terminal domains (C0-C1-motif-C2) of

cardiac (c) MyBP-C to affect actomyosin interactions and to interact with actin. Recombinant proteins containing the C1 and motif domains increased  $\text{Ca}^{2+}$  sensitivity of tension and increased rates of tension redevelopment ( $k_{tr}$ ) at submaximal  $[\text{Ca}^{2+}]$  in permeabilized rat trabeculae. Proteins containing these domains also biphasically activated and then inhibited the  $\text{Ca}^{2+}$ -activated ATPase rates of heavy meromyosin and myosin S1 in solution. Cosedimentation binding assays demonstrated binding of the four N-terminal domains to F-actin at a 1:1 molar ratio ( $K_d \sim 10$   $\mu$ M). Phosphorylation of the motif reduced binding to a 1:2 molar ratio but did not completely eliminate the effects of recombinant proteins to increase  $\text{Ca}^{2+}$  sensitivity of tension and  $k_{tr}$  at submaximal  $[\text{Ca}^{2+}]$  in permeabilized trabeculae. We propose that the functional effects of cMyBP-C are mediated in part through phosphorylation-sensitive interactions with the thin filament.

Supported by NIH HL080367.

#### 9. Developing the Hypothesis That Dysferlin Is Required for Stabilizing Muscle T-Tubule Connections to the Sarcolemma. **JOHN HEUSER, LUCY LOULTCHEVA, TANYA TENKOVA, and ROBYN ROTH, Department of Cell Biology, Washington University School of Medicine, St. Louis, MO 63110, and Institute for Integrated Cell-Material Sciences (iCeMS), Kyoto University, Kyoto 606-8501, Japan**

We will advance the hypothesis in this poster that muscle T-tubules are uniquely vulnerable to damage during eccentric contractions, and that the muscle protein dysferlin plays a special role in stabilizing T-tubule connections with the plasma membrane, or reestablishing connections with the plasma membrane if and when T-tubules are damaged by this sort of contraction. Further, we will illustrate that the reason for this T-tubule vulnerability, which is unique to muscle, is due to the fact that the surface membrane of the muscle fiber, the sarcolemma, is pinned down to the special extracellular matrix that surrounds all muscle fibers and stabilizes them, so the surface membrane cannot slip laterally. We will then illustrate how the T-tubule system, which connects everywhere to the sarcolemma to spread excitation throughout the muscle fiber, is itself pinned down to certain positions in the myofilament lattice of the internal sarcoplasmic contractile apparatus. These competing physical constraints, we will argue, mean that whenever the internal myofilament lattice becomes displaced laterally from its natural starting point distribution relative to the surrounding sarcolemma (as it likely does during eccentric contraction), the T-tubule origins and insertions must become stretched and, consequently, T-tubules become vulnerable to rupture or evulsion from the cell surface. We will further illustrate how and why this sort of T-tubule evulsion would interrupt excitation-contraction coupling in the affected

region of the muscle fiber and likely cause a local flaccid paralysis, which could promote further plasmalemmal/sarcomere dislocation and further T-tubule rupture, thus propagating the muscle damage. Finally, we will conclude that if dysferlin is not the protein that helps to prevent such T-tubule damage or helps to heal it, discovering whatever protein does do this job will become just as important for understanding all the muscular dystrophies as is understanding the role of dysferlin itself.

10. Configuration of Myosin-binding Protein C in Skeletal Muscle. HUGH E. HUXLEY,<sup>1</sup> MASSIMO RECONDITI,<sup>2</sup> and THOMAS IRVING,<sup>3</sup> <sup>1</sup>*Rosenstiel Center, Brandeis University, Waltham, MA 02453;* <sup>2</sup>*Physiology Department, University of Florence, 50019 Sesto Fiorentino, Italy;* <sup>3</sup>*IIT Chicago and BioCAT, APS Argonne National Laboratory, Argonne, IL 60439*

Frog striated muscle gives a pair of x-ray meridional reflections at the spacings of  $\sim$ 419 and  $\sim$ 442 Å, which Offer (CSH Symp. 1972. 37:83–97) and Rome (ibid., 331–339) have shown are related to the disposition of C protein in two sets of bands at  $\sim$ 430-Å intervals on either side of the H-zone, giving rise to interference fringes that sample the underlying 430-Å reflection. However, there are problems with this simple interpretation.

We have studied these reflections at high resolution on the BioCAT beam line at the Argonne National Laboratory, in both relaxed and contracting muscles, and during the onset of activation. In resting muscle, two main peaks can generally be seen in the relevant region, and usually at  $\sim$ 419 and  $\sim$ 442 Å as previously described, but the latter peak is approximately four times more intense than the former, which would require an underlying sampled peak at  $\sim$ 437 Å. It seems very unlikely that the C protein repeat is different from that of the myosin filament to which it is attached (429.6 Å), although Squire et al. (Squire, J.M., P.K. Luther, and C. Knupp. 2003. *J. Mol. Biol.* 331:713–724) have suggested that C protein may interact in relaxed muscle with specific sites on actin to produce such an effect. We think another explanation is more probable, namely a double-interference effect.

The second component would be a “forbidden” first-order myosin reflection, as discussed by Malinchik and Lednev (Malinchik, S.B., and V.V. Lednev. 1992. *J. Muscle Res. Cell Motil.* 13:406–419), arising because of systematic axial displacements of myosin cross-bridges (average repeat of 143.2 Å) within the 429.6-Å helical repeat. The interference fringes generated by this system would interact in a complex way with those from C protein because the reflections would in general have different phases. We find that the observed pattern, with the very strong  $\sim$ 442-Å reflection, can be modeled very satisfactorily, even when both underlying peaks are kept at 429.6 Å.

Some other relevant observations are also described.

11. A Contraction-dependent Pathway Regulates Myofibril Organization during Skeletal Muscle Development In Vivo. MANUELA LAHNE, CHRISTINA KRIVCEVSKA, and RACHEL ASHWORTH, *Queen Mary University of London, School of Biological and Chemical Sciences, London E1 3NS, England, UK*

The earliest movements (17–22 hpf) in zebrafish embryos are characterized by spontaneous muscle contractions driven via acetylcholine-generated  $\text{Ca}^{2+}$  signals. Mutant lines lacking key components of the excitation–contraction (E-C) pathway, the acetylcholine receptor, and the dihydropyridine receptor (DHPR) show disrupted skeletal muscle development, specifically shorter sarcomeres and longer, misaligned myofibrils (Brennan, C., M. Mangoli, C.E.F. Dyer, and R. Ashworth. 2005. *J. Cell Sci.* 118:5181–5190). Based on evidence from these mutants, we propose that myofibril organization is controlled downstream of membrane depolarization. The underlying intracellular signaling mechanisms are currently still unknown.  $\text{Ca}^{2+}$ -mediated muscle contraction or  $\text{Ca}^{2+}$  signals acting independently of contraction could be involved in myofibril organization downstream of membrane depolarization. To distinguish between these two mechanisms, we used a pharmacological approach using the myosin II inhibitor blebbistatin to block muscle contraction. Movement was blocked for a period of 7 hours starting at 17 hpf, and skeletal muscle morphology was subsequently examined using immunocytochemistry. Slow muscle fibers of blebbistatin-treated embryos (10, 50  $\mu\text{M}$ ) displayed misaligned myofibrils similar to the mutants lacking E-C coupling, suggesting that muscle contraction is a critical regulatory step. However, as blebbistatin inhibits both muscle and non-muscle myosin II, it might affect not only muscle fiber but also neuronal development. Axon outgrowth was similar in control and blebbistatin-treated embryos, but an apparent increase in neurite number and the loss of varicosities were observed. Disruption to the neuronal pathfinding might affect E-C coupling upstream of contraction and be the underlying cause of the myofiber phenotype. Assessment of functional neuromuscular communication by measurement of  $\text{Ca}^{2+}$  signals in muscle fibers revealed that E-C coupling remained intact. Collectively, our data suggest that a functional contractile apparatus is required for myofibril organization. The late steps of muscle differentiation that rely upon embryonic movement may be regulated by a novel contractile-dependent mechanism.

12. Integration of Signaling at the Level of Sarcomeres with Electrical and Metabolic Signaling in the Heart. R. JOHN SOLARO, *Department of Physiology and Biophysics, University of Illinois at Chicago, College of Medicine, Chicago, IL 60612*

Emerging evidence indicates that beyond their role as molecular motors, sarcomeric proteins are important

in efficient coordination of electrical, mechanical, and chemical signals and the matching of energy demand to energy supply. Sarcomeric proteins sense mechanical, chemical, and redox state and serve as sites of signal reception from G protein-coupled receptors and intracellular G protein-controlled processes. In turn, sarcomeric proteins—especially at the Z-disk—participate in signal transduction by acting as docking and shuttle sites for kinases, phosphatases, and transcription factors. Signaling and signal transduction at the level of sarcomeres control cardiac dynamics, growth, and remodeling. Mechano-electrical feedback is also now understood to involve  $\text{Ca}^{2+}$  ions buffered by sarcomeric proteins. Recent evidence also demonstrates linkages among elements in control of metabolic activity and sarcomeric function. For example, kinases such as PKD and AMP kinase not only regulate metabolic pathways, but also affect sarcomeric response to  $\text{Ca}^{2+}$ . The challenge is to fully integrate these signaling processes at the level of sarcomeric proteins with signaling at the level of channels, transporters, and exchangers, as well as elements controlling redox state and metabolism. Disturbances in the role of sarcomeric proteins in integration of these processes represent a significant threat to homeostasis. There are no better examples of this threat than familial cardiomyopathies genetically linked to mutations in sarcomeric proteins. It is highly likely that these disturbances are also significant in acquired cardiac disorders. There are promising data indicating that sarcomeric proteins are useful as therapeutic targets in the treatment of cardiac disorders. These findings demand more complete understanding of the processes in sarcomeric signaling from the molecular, cellular, organ, and whole body levels.

### SESSION III: CALCIUM SIGNALING

13. Altered Skeletal Muscle L-type  $\text{Ca}^{2+}$  Channel Activity in RyR1 R163C Malignant Hyperthermia-susceptible Mice. R.A. BANNISTER,<sup>1</sup> E. ESTÈVE,<sup>2</sup> K. LIU<sup>2</sup>, J.M. ELITIT,<sup>2</sup> P.D. ALLEN,<sup>2</sup> I.N. PESSAH,<sup>3</sup> J. LÓPEZ,<sup>2</sup> and K.G. BEAM,<sup>1</sup> <sup>1</sup>*Department of Physiology and Biophysics, University of Colorado-Denver, Aurora, CO 80045; <sup>2</sup>Department of Anesthesiology, Perioperative and Pain Medicine, Brigham and Women's Hospital, Boston, MA 02115; <sup>3</sup>Department of Molecular Biosciences, School of Veterinary Medicine, University of California, Davis, Davis, CA 95616*

In skeletal muscle, intermolecular communication between the L-type  $\text{Ca}^{2+}$  channel (1,4-dihydropyridine receptor [DHPR]) and the type 1 ryanodine receptor (RyR1) is bidirectional; orthograde coupling is observed as depolarization-induced  $\text{Ca}^{2+}$  release from the sarcoplasmic reticulum, and retrograde coupling is manifested by increased L-type  $\text{Ca}^{2+}$  current. The pharmacogenetic disorder malignant hyperthermia

(MH), which is triggered by exposure to heat, volatile anaesthetics, or depolarizing muscle relaxants, has been linked to >120 mutations in RyR1. In this study, we investigated whether DHPR activity is affected by one of these MH-linked mutations in RyR1 (R163C). To this effect, the I-V relationship for L-type currents in myotubes originating from R163C mice was shifted to more hyperpolarizing potentials ( $\sim 5$  and 7 mV for HET and HOM, respectively) compared with wild-type myotubes ( $P < 0.001$ ; ANOVA). Compared with wild-type myotubes, R163C HET and HOM myotubes both displayed a greater sensitivity to the 1,4-dihydropyridine agonist  $\pm$ Bay K 8644 (10  $\mu\text{M}$ ). Intramembrane charge movements of both HET and HOM myotubes were profoundly shifted ( $>10$  mV) to more hyperpolarized potentials ( $P < 0.005$ ; ANOVA). L-type currents in wild-type and HET myotubes displayed only modest (<35%) inactivation after 30-s prepulses to  $-50$ ,  $-30$ , and  $-10$  mV, with no apparent difference between the two genotypes. Our results demonstrate that the RyR1 R163C mutation alters the voltage dependence of L-type channel activity and suggest that this hypersensitivity to membrane potential contributes to increased myoplasmic  $\text{Ca}^{2+}$  levels associated with MH episodes.

Supported by NIH NS24444 and AR44750 to K.G. Beam, NIH AR052354 to P.D. Allen, and MDA 4155 to R.A. Bannister.

14. Cardiac  $\text{Ca}^{2+}$  Cycling in Health and Arrhythmias. DAVID EISNER, TAKESHI KASHIMURA, LUIGI VENETUCCI, and ANDREW TRAFFORD, *Unit of Cardiac Physiology, The University of Manchester, Core Technology Facility, Manchester M13 9NT, England, UK*

Most of the calcium that activates contraction in the ventricle comes from the sarcoplasmic reticulum (SR) and is released by the process of calcium-induced calcium release (CICR). I will initially consider the mechanisms involved in regulating SR Ca content. We find a simple feedback mechanism in which an increase of SR Ca results in a larger systolic Ca transient that, in turn, increases Ca efflux from the cell, thereby decreasing SR Ca content. One consequence of this feedback is that maneuvers that increase the open probability of the RyR do not produce a maintained increase of systolic Ca.

If SR Ca content is increased above a threshold value, propagating waves of CICR are observed. These waves produce arrhythmogenic delayed afterdepolarizations (DADs) by activating the electrogenic NCX. This may also occur when SR Ca content is not elevated. One example is in the presence of mutations of the RyR that can cause catecholaminergic polymorphic ventricular tachycardia (CPVT). Here, ventricular arrhythmias occur when catecholamine levels are increased during exercise and other stresses. This arises because the mutated RyRs leak Ca during diastole.

We have examined whether increasing the RyR leak per se produces diastolic Ca waves. When low concentrations of caffeine are applied to increase RyR opening, Ca waves are only seen for a few seconds. The disappearance of the Ca waves is due to the accompanying decrease of SR Ca content. If, however, a  $\beta$ -adrenergic agonist is first applied, caffeine produces waves in the steady state and we attribute this to the increase of SR Ca content due to the  $\beta$  agonist. This explains why the patients with mutated RyRs develop arrhythmias during exercise.

The final part of the talk will consider how Ca wave-dependent arrhythmias might be treated. We find that decreasing the open probability of the RyR with tetracaine abolishes the Ca wave and increases the systolic Ca release.

15. Changes in  $\text{Ca}^{2+}$  Transients and Phasic Contractions Induced by Uropathogenic *E. coli* (UPEC) in Smooth Muscle of the Rat Ureter. RACHEL V. FLOYD,<sup>1</sup> ALI BAKRAN,<sup>2</sup> CRAIG WINSTANLEY,<sup>3</sup> SUSAN WRAY,<sup>1</sup> and TED BURDYGA,<sup>1</sup> <sup>1</sup>*Department of Physiology, <sup>2</sup>Vascular and Transplant Surgery Unit, Royal Liverpool University Hospital, and <sup>3</sup>Division of Medical Microbiology and GU Medicine, University of Liverpool, Liverpool L69 3BX, England, UK*

Urinary tract infection (UTI) remains a significant cause of postoperative complications after renal transplant surgery and is the second most common infection seen in general practice. UTI, therefore, remains a constant and important clinical as well as economic problem. Ascending UTIs cause abnormal ureteric function, but little is known about the mechanisms causing this effect. Our preliminary studies have shown that prolonged intraluminal exposure of rat ureter to UPEC caused changes in ureteric smooth muscle contractility; however, the underlying mechanisms causing this effect were unclear. In the present study, changes in phasic contractions and  $\text{Ca}^{2+}$  transients evoked by electrical field stimulation of Indo-1-loaded rat ureters during exposure to UPEC were investigated. Exposure of ureters to pathogenic UPEC J96 on the luminal but not adventitial side of the ureter caused a time-dependent decrease in amplitude and duration of the  $\text{Ca}^{2+}$  transient and phasic contractions. Nonpathogenic TG2 under identical conditions had little or no effect. Inhibition of  $\text{K}^+$  channels by TEA (5 mM) significantly but not completely reversed the inhibitory effects of J96 on  $\text{Ca}^{2+}$  transients and force. J96 also decreased  $\text{Ca}^{2+}$  transients and force induced by sustained high- $\text{K}^+$  depolarization. Our data indicate that a decrease in the amplitude of the phasic contractions induced by prolonged exposure to J96 in rat ureter smooth muscle is associated with a decrease in the amplitude and duration of the  $\text{Ca}^{2+}$  transient. The data suggest that this modulation of the  $\text{Ca}^{2+}$  transient and force in rat ureter smooth muscle induced by intraluminal J96 exposure is likely associated with an up-regulation of the activity of potassium channels and down-regulation of the activity of L-type calcium channels.

16. Structure–Function Relationships in Calcium Release Units. CLARA FRANZINI-ARMSTRONG, *Department of Cell and Developmental Biology, University of Pennsylvania, Philadelphia, PA 19104*

The junctional domain of sarcoplasmic reticulum (jSR) is specialized for receiving signals from the plasmalemma/transverse tubules and for releasing  $\text{Ca}^{2+}$  during muscle activation. The junctional face of the jSR, facing the T tubules, is occupied by a molecular complex composed of the transmembrane  $\text{Ca}^{2+}$  release channels (ryanodine receptors [RyRs]), the luminal protein calsequestrin (CSQ), the two membrane proteins, junctin and triadin (Jct, Tr), which mediate CSQ–RyR interactions, and several other components. Under the conditions prevailing within the SR lumen (physiological ionic strength, mostly due to  $\text{K}^+$   $\text{Ca}^{2+}$  ions), CSQ forms long linear polymers, and the fixed protein gel is clearly visible in the electron microscope. The luminal domains of Jct and Tr are detectable, but overall the two molecules are not clearly delineated. Overexpression and/or null mutation for the three proteins of the junctional complex (CSQ, Jct, and Tr) in skeletal and cardiac muscles reveal the contribution of these three components to the general architecture and maintenance of the jSR.

17. P2X Receptor–mediated Current in Myocytes from Renal Resistance Arteries. MAKSYM HARHUN,<sup>1</sup> OLEK-SANDR POVSTYAN,<sup>1,2</sup> and DMITRI GORDIENKO,<sup>1,2</sup> <sup>1</sup>*Ion Channel and Cell Signaling Centre, Division of Basic Medical Sciences, St George's, University of London, London SW17 ORE, England, UK; <sup>2</sup>Laboratory of Molecular Pharmacology and Biophysics of Cell Signaling, Bogomoletz Institute of Physiology, Kyiv 01024, Ukraine*

Activation of ionotropic P2X purinoreceptors (P2XRs) elevates  $[\text{Ca}^{2+}]_i$  in renal vascular smooth muscle cells (RVSMCs) triggering their contraction, thus, leading to renal vasoconstriction (Inscho, E.W. 2001. *Am. J. Physiol. Renal Physiol.* 280:F927–F944). By combining perforated patch tight-seal recording with confocal  $\text{Ca}^{2+}$  imaging (with fluo-4), we related the dynamics of  $[\text{Ca}^{2+}]_i$  mobilization to the kinetics of P2XR-mediated cationic current ( $I_{\text{P2X}}$ ) or changes in the membrane potential of RVSMCs freshly isolated from interlobar and arcuate arteries of rat kidney and stimulated with 10  $\mu\text{M}$   $\alpha, \beta$ -methyleneadenosine triphosphate (AMP-CPP). Under current clamp, spike-like depolarization was associated with transient  $[\text{Ca}^{2+}]_i$  mobilization. Under voltage clamp, the  $[\text{Ca}^{2+}]_i$  transient was associated with  $I_{\text{P2X}}$  activation: the current density was  $141.5 \pm 10.5 \text{ pA/pF}$  ( $n = 38$ ) at  $V_h = -60 \text{ mV}$ . Both spike-like depolarization and  $I_{\text{P2X}}$  peaked before  $[\text{Ca}^{2+}]_i$  reached its maximum, suggesting that  $I_{\text{P2X}}$  is a major determinant of the spike-like depolarization, and that there are other than  $I_{\text{P2X}}$  contributors to the  $[\text{Ca}^{2+}]_i$  transient. RT-PCR analysis conducted on 500 isolated RVSMCs showed the presence

of genes encoding P2X<sub>1</sub>R and P2X<sub>4</sub>R. Concentration dependence of I<sub>P2X</sub> activation with AMP-CPP revealed EC<sub>50</sub> = 1.1 ± 0.1 μM (n = 6–7). I<sub>P2X</sub> induced by 10 μM AMP-CPP completely recovered from desensitization within 7 min. An increase in extracellular Ca<sup>2+</sup> from 1 to 5 mM reduced I<sub>P2X</sub> by 48 ± 6% (n = 5). Nanomolar concentrations of NF279 (selective inhibitor of P2X<sub>1</sub>R) reduced I<sub>P2X</sub> by 68 ± 3% in a concentration-dependent manner (EC<sub>50</sub> = 8 ± 3 nM; n = 5–6). The residual current was virtually insensitive to intermediate concentrations (0.2–20 μM) of NF279, but was inhibited with 2 mM NF279. This study provides strong evidence that in rat RVSNCs, I<sub>P2X</sub> is mediated by at least two P2XRs subtypes: P2X<sub>1</sub>R and P2X<sub>4</sub>R.

This work was supported by BHF (PG/08/062/25382 and FS/06/077).

18. Increase of Ryanodine Receptor Type-2 (RyR2) mRNA via an Activation of Ca<sub>v</sub>1.3 Liter-type Ca<sup>2+</sup> Channels. SUNOH KIM and HYEWHON RHIM, *Life Sciences Division, Korea Institute of Science and Technology (KIST), Seoul 136-791, Korea*

Ryanodine receptors (RyRs) are extremely important for triggering muscle contraction and physically linked with L-type Ca<sup>2+</sup> channels, providing an amplification of the Ca<sup>2+</sup> signal necessary to trigger muscle contraction. However, this coupling between L-type Ca<sup>2+</sup> channels and RyRs has not been well characterized in the CNS. In this study, we used a yeast two-hybrid screening system with the N terminus of rat Ca<sub>v</sub>1.3 α<sub>1</sub> subunit (Ca<sub>v</sub>1.3-NT) as bait and isolated a partial N-terminal amino acid sequence of RyR type 2 (RyR2-NT) as a binding partner. We also demonstrated a physical association of Ca<sub>v</sub>1.3 with RyR2 using GST pull-down, coimmunoprecipitation, and immunocytochemistry assays. Depolarizing cells showed that the activation of L-type Ca<sup>2+</sup> channels induced RyR opening and led to RyR-dependent Ca<sup>2+</sup> release, even in the absence of extracellular Ca<sup>2+</sup>. Furthermore, we found that RyR2 mRNA itself is increased by long-term treatment of high-K via activation of L-type Ca<sup>2+</sup> channels. These acute and long-term effects of high-K on RyRs were selectively blocked by small interfering RNA-mediated silencing of Ca<sub>v</sub>1.3. These results suggest a physical and functional interaction between Ca<sub>v</sub>1.3 and RyR2 and important implications of Ca<sub>v</sub>1.3/RyR2 clusters in translating synaptic activity into alterations in gene expression.

This work was supported by KIST Core-Competence Program, Brain Research Center of the 21st Century Frontier Research Program, and the KOSEF grant.

19. Combined Mathematical Model of Electrical and Mechanical Activity of Ventricular Cardiomyocytes in Rat. P. KONOVALOV, O. SOLOVYOVA, L. KATSNELSON, and V.S. MARKHASIN, *Institute of Immunology and*

*Physiology, Ural Division of the Russian Academy of Sciences, Yekaterinburg 620219, Russia*

Previously, we have developed a mathematical model of the rat ventricular cardiomyocyte mechanical activity (Katsnelson, L.B., L.V. Nikitina, D. Chemla, O. Solovyova, C. Coirault, Y. Lecarpentier, and V.S. Markhasin. 2004. *J. Theor. Biol.* 230:385–405) that simulated a wide range of experimental phenomena, including load dependence of relaxation, muscle inactivation due to the length change, and mechanical effects on Ca<sup>2+</sup> transient in cardiomyocytes. The model was further parametrically fitted to the guinea pig mechanics and combined with the Noble'98 model of guinea pig electrophysiology. It proved to simulate major effects of cardiac mechano-electric feedback (Solovyova, O., N. Vikulova, L.B. Katsnelson, V.S. Markhasin, P.J. Noble, A. Garry, P. Kohl, and D. Noble. 2003. *Inter. J. Bifurcation and Chaos*. 13:3757–3782; T. Sulman, L.B. Katsnelson, O. Solovyova, and V.S. Markhasin. 2008. *Bull. Math. Biol.* 70:910–949). Moreover, the model was successfully used in both theoretical and experimental models of cardiac heterogeneity (*ibidem*), particularly within our hybrid muscle duplex approach (Y.L. Protsenko, S.M. Routkevitch, V.Y. Gur'ev, L.B. Katsnelson, O. Solovyova, O.N. Lookin, A.A. Balakin, P. Kohl, and V.S. Markhasin. 2005. *Am. J. Physiol. Heart Circ. Physiol.* 289:H2733–H2746), where mechanical interaction between real and virtual muscles was implemented in real time. These reasons make us combine our rat mechanical model and a model of rat electrophysiology (S.V. PandZit, R.B. Clark, W.R. Giles, and S.S. Demir. 2001. *Biophys. J.* 81:3029–3051), as rat is a commonly used experimental species. However, this new electro-mechanical model initially was not adequate. Particularly, the model revealed Ca<sup>2+</sup> overload of the cell when pacing at 1, 0.5, and 0.3 Hz. Moreover, the ratio between amounts of Ca<sup>2+</sup> released from the SR and entering the cell via L-type channels was not realistic and did not allow us to simulate contractions properly. Both inadequacies happened due to the equations for Ca<sup>2+</sup> exchange between the SR and cytosol adopted from the Pandit's model. Therefore, we completely replaced Pandit's description of Ca<sup>2+</sup> handling with that from our model and fitted several parameters. The combined model is now able to simulate correctly both electrical and mechanical cardiac performance in rat.

This work is supported by RFBR grants 08-04-01137 and 07-04-96113, and a UBRAS multidisciplinary grant.

20. The Mechanism of Myogenic Control of Arterial Diameter via Ca<sup>2+</sup> Sensitization. MICHAEL P. WALSH, ROSALYN P. JOHNSON, AHMED F. EL-YAZBI, KOSUKE TAKEYA, EMMA J. WALSH, and WILLIAM C. COLE, *The Smooth Muscle Research Group, Faculty of Medicine, University of Calgary, Calgary, Alberta, Canada T2N 1N4*

Contraction of resistance arteries in response to increased transmural pressure (the myogenic response)

is a crucial determinant of peripheral vascular resistance, blood pressure, and regional blood flow control in several vascular beds, including the cerebral vasculature. Understanding of the molecular mechanisms involved in the myogenic response, however, is incomplete. Myogenic constriction is dependent in part on pressure-induced membrane potential depolarization, but mechanisms in addition to changes in membrane potential and cytosolic free  $\text{Ca}^{2+}$  concentration ( $[\text{Ca}^{2+}]_i$ ) have been implicated. For example,  $\text{Ca}^{2+}$  sensitization, i.e., an increase in force without a change in  $[\text{Ca}^{2+}]_i$ , has been suggested to contribute to the myogenic response, but the underlying mechanism remains to be elucidated. We investigated the potential involvement of Rho-associated kinase (ROK)- and protein kinase C (PKC)-dependent phosphorylation of the myosin light chain phosphatase-targeting subunit (MYPT1) and of the 17-kD PKC-potentiated protein phosphatase 1 inhibitor protein (CPI-17), respectively, in the myogenic response of rat middle cerebral arteries. Inhibitors of ROK (Y27632 and H1152) and PKC (GF109203X and Gö6976) suppressed the myogenic response. Elevated pressure (60 and 100 mmHg vs. 10 mmHg) increased phosphorylation of MYPT1 at T855, but not T697, and enhanced myosin regulatory light chain ( $\text{LC}_{20}$ ) phosphorylation in an H1152-sensitive manner. However, pressure did not evoke CPI-17 phosphorylation, and inhibition of PKC did not affect the pressure-induced increases in MYPT1 (T855) or  $\text{LC}_{20}$  phosphorylation. Our findings provide the first direct biochemical evidence that  $\text{Ca}^{2+}$  sensitization induced by ROK-dependent phosphorylation of MYPT1 at T855 (but not T697), with subsequent augmentation of  $\text{LC}_{20}$  phosphorylation and force generation, contributes to the myogenic response in the cerebral vasculature. On the other hand, suppression of the myogenic response by PKC inhibition cannot be attributed to block of  $\text{Ca}^{2+}$  sensitization mediated by CPI-17 or MYPT1 phosphorylation.

Supported by grant MOP-10568 from the Canadian Institutes of Health Research.

#### SESSION IV: DISEASE AND REPAIR

21. Stretch-induced Muscle Damage and Duchenne Muscular Dystrophy. **D.G. ALLEN**,<sup>1</sup> O.L. GERVASIO,<sup>1</sup> E.W. YEUNG,<sup>2</sup> and N.P. WHITEHEAD<sup>1</sup>, <sup>1</sup>*School of Medical Sciences and Bosch Institute, University of Sydney, Sydney, NSW 2006, Australia; <sup>2</sup>Department of Rehabilitation Sciences, Hong Kong Polytechnic University, Hung Hom, Kowloon, Hong Kong*

Duchenne muscular dystrophy is a severe muscle wasting disease caused by the absence of the cytoskeletal protein dystrophin. Experiments on the *mdx* mouse, which also lacks dystrophin, have shown that *mdx* muscles are particularly susceptible to stretch-induced damage. We

have shown that  $\text{Ca}^{2+}$  entry through a channel blocked by streptomycin,  $\text{Gd}^{3+}$ , or the spider venom peptide, GsMTx-4, contributes to stretch-induced muscle damage (Yeung, E.W., N.P. Whitehead, T.M. Suchyna, P.A. Gottlieb, F. Sachs, and D.G. Allen. 2005. *J. Physiol.* 562:367–380). The pharmacological and functional properties of this  $\text{Ca}^{2+}$  entry channel resemble a stretch-activated channel permeable to many cations known as  $\text{SAC}_{\text{NSC}}$ , which is expressed in muscle and for which a candidate gene is TRPC1 (Maroto, R., A. Raso, T.G. Wood, A. Kurosky, B. Martinac, and O.P. Hamill. 2005. *Nat. Cell Biol.* 7:179–185). We have also shown that  $\text{Ca}^{2+}$  entry into *mdx* muscle fibers can also be stimulated by  $\text{H}_2\text{O}_2$  and entry is also blocked by streptomycin, suggesting that the physiological activator of  $\text{SAC}_{\text{NSC}}$  may be reactive oxygen species (ROS). To gain further understanding of the properties of TRPC1, it was expressed in C2 myoblasts. When expressed alone, it did not appear in the surface membrane, but when coexpressed with caveolin-3, the proteins co-located in the membrane (Gervásio, O.L., N.P. Whitehead, E.W. Yeung, W.D. Phillips, and D.G. Allen. 2008. *J. Cell Sci.* 121:2246–2255). When TRPC1 was located in the membrane, it could be activated by  $\text{H}_2\text{O}_2$ , causing  $\text{Ca}^{2+}$  influx that was blocked by PP2, an inhibitor of src kinase. These data suggest that in muscular dystrophy, excessive production of ROS might open  $\text{SAC}_{\text{NSC}}$  channels by activating src kinase. These pathways offer several new targets for therapy of muscular dystrophy.

22. Displacement Currents and Voltage Dependency of Bi-stable Reversible Transitions in Molluscan Rhodopsin. MARÍA DEL PILAR GOMEZ<sup>1,3</sup> and ENRICO NASI,<sup>2,3</sup> <sup>1</sup>*Departamento de Biología* and <sup>2</sup>*Instituto de Genética, Universidad Nacional de Colombia, Bogotá; <sup>3</sup>Marine Biological Laboratory, Woods Hole, MA 02543*

The molecular rearrangement of rhodopsin upon photoisomerization is accompanied by a net charge displacement with a vectorial component normal to the membrane plane. As a result, a rapid early receptor current (ERC) is produced, which is easily detectable by voltage clamp recording when the photopigment is embedded in the plasmalemma. This signal allows, among others, separating the triggering events of the visual process from those arising from the subsequent activation of the enzymatic transduction pathway. We examined the ERC in the ciliary photoreceptors of the distal retina of *Pecten*, in which the photopigment is thermally stable, and transitions between rhodopsin (R) and metarhodopsin (M) states are accompanied by a marked shift in spectral absorbance; as such, reversible manipulations of the pigment-state distribution can be induced by chromatic illumination. Delivery of brief, intense flashes under voltage clamp induced displacement currents that could be isolated by kinetics, by pharmacological blockage of the photoconductance, or

by elimination of the driving force on K ions that comprise the photocurrent. The polarity and amplitude of the displacement currents could be controlled by prior chromatic adaptation in which the wavelength of the adapting light was varied, while using fixed, spectrally neutral test stimuli. In particular, limiting initial distributions yielded ERCs of opposite directions (concomitant with M→R and R→M transitions, respectively), but conserved total charge. The occurrence of a charge displacement necessarily implies that the conformational transition rates of the receptor molecule must interact with the membrane field. We recorded ERCs in both directions, while systematically varying the holding potential of the cell by voltage clamp. A distinct, orderly dependency of the peak amplitude of the displacement current on membrane potential was obtained; this relation is analyzed in terms of energetics of rhodopsin conformational rearrangement and the equivalent charge implicated.

Supported by NSF grant 0639774.

23. Extending the Sensitivity of Amperometric Recording By Phase-Lock Measurements. MARÍA DEL PILAR GÓMEZ,<sup>1,4</sup> JUAN MANUEL ANGUEYRA,<sup>2,4</sup> and ENRICO NASI,<sup>3,4</sup> <sup>1</sup>Departamento de Biología, <sup>2</sup>Programa de Neurociencias, and <sup>3</sup>Instituto de Genética, Universidad Nacional de Colombia, Bogotá; <sup>4</sup>Marine Biological Laboratory, Woods Hole, MA 02543

Electrochemical detection of oxidizable compounds via microscopic fibers has been a valuable approach for examining secretion mechanisms, and, in its most ambitious applications, has allowed monitoring release at the single-cell level. Inevitably, owing to the minute amounts of the target substance, concentration changes in the vicinity of an individual, isolated cell are exceedingly small, and the sensitivity limit of the detecting instrument is a severe limiting factor. This issue is particularly challenging for non-vesicular secretion, a non-canonical mechanism of significant interest: unlike exocytosis (where the molecules are released in batches of thousands), in this case extrusion occurs at a much slower rate, and the resulting extracellular concentration changes are even smaller, yielding a grossly inadequate signal-to-noise ratio. Phase-locked detection can bring out a small signal buried in a much larger noise, provided that the signal in question can be modulated with an established periodicity, which effectively accomplishes two goals: (1) displace the signal away from the DC end of the spectrum, where 1/f noise is dominant; (2) enable extraction of the signal by ultra-narrow bandwidth filtering. We developed a method in which the electrical potential of a carbon fiber is modulated sinusoidally, and a dual phase/lock loop amplifier is used to extract the oxidation current from contaminating dielectric signals of the same frequency that arise from the electrical double-layer at the electrode–solution inter-

face. The bandwidth of this approach is limited by the integration interval and thus by the driving frequency used. Initial measurements reveal that the detection limit attained exceeds that of conventional amperometric measurements with constant electrode polarization, while the temporal resolution is in the range of  $10^{-1}$  s. This approach can thus be useful for point measurements of changes in concentration of oxidizable substances released with flux magnitudes and time course like those expected in transporter-mediated extrusion.

24. Skeletal Muscle Impairment during Microgravity-induced Disuse: Beneficial Effects of Different Pharmacological Countermeasures. J.-F. DESAPHY,<sup>1</sup> A. LIANTONIO,<sup>1</sup> S. PIERNO,<sup>1</sup> C. DIGENNARO,<sup>1</sup> V. CIPPONE,<sup>1</sup> G. CAMERINO,<sup>1</sup> V. GIANNUZZI,<sup>1</sup> S. SIMONETTI,<sup>2</sup> and D. CONTE CAMERINO,<sup>1</sup> <sup>1</sup>Sezione di Farmacologia, Dip. Farmaco-biologico, Facoltà di Farmacia, Università degli Studi di Bari, 70124 Bari, Italy; <sup>2</sup>Laboratorio Analisi, Diagnostica Biochimica Metabolica, Ospedale Giovanni XXIII, 70126 Bari, Italy

Rodent hindlimb unloading (HU) is a widely accepted ground-based model of skeletal muscle adaptation to microgravity or bed rest–induced disuse. After HU, soleus muscle, a slow-twitch muscle functionally devoted to postural maintenance, experience atrophy and slow-to-fast phenotype transition. In parallel, resting sarcolemma chloride conductance (gCl), which controls muscle excitability, and cytosolic calcium at rest (restCa) are modified by HU condition. Indeed, restCa, measured by FURA-2, decreased and gCl, measured by 2-intracellular-microelectrode current clamp technique, increased after 3-day HU toward values typical of fast-twitch muscle, before initiation of myosin heavy chain (MHC) transition. The gCl increase resulted from the reduction of protein kinase C activity (Pierno, S., J.F. Desaphy, A. Liantonio, A. De Luca, A. Zarrilli, L. Mastrofrancesco, G. Procino, G. Valenti, and D. Conte Camerino. 2007. *J. Physiol.* 584:983–995). In soleus muscle of 14-day HU rodents, the expression of fast MHC isoform was also found to be increased. Searching for potential candidates able to counteract muscle alterations, we tested drugs able to affect those parameters modified by HU. The aminoacid taurine is known to modulate both calcium homeostasis and gCl (Conte Camerino, D., D. Tricarico, S. Pierno, J.F. Desaphy, A. Liantonio, M. Pusch, R. Burdi, C. Camerino, B. Fraysse, and A. De Luca. 2004. *Neurochem. Res.* 29:135–142). A taurine-enriched diet significantly prevented changes in gCl, restCa, and MHC expression, but not atrophy in HU rat soleus muscles. Recent data suggest a link between oxidative stress and muscle atrophy. Thus, we evaluate the effects of the treatment with the potent antioxidant trolox in HU mice. This compound fully prevented lipid peroxidation, measured by fluorimetric technique and gCl increase. However, trolox partially counteracted

MHC isoform transition, but had no effect on atrophy. The hormone ghrelin can improve lean body mass in catabolic states and reduces gCl in fast-twitch muscles through PKC activation. Preliminary experiments suggest that ghrelin improves the modification of gCl in soleus muscle of 3–14-day HU mice. These results demonstrate the beneficial effects of all these compounds in the prevention of HU-induced muscle impairment.

Supported by ASI-OSMA.

**25. Calcium, MAPKs, and Cardiac Hypertrophy.** FAYE M. DRAWNEL<sup>1</sup> and H. LLEWELYN RODERICK,<sup>1,2</sup> *<sup>1</sup>Laboratory of Molecular Signaling, Babraham Institute, Cambridge CB22 3AT, England, UK; <sup>2</sup>Department of Pharmacology, University of Cambridge, Cambridge CB2 1PD, England, UK*

Pathological cardiac hypertrophy is a maladaptive response of the myocardium to persistent cardiovascular stress. The cellular features observed during hypertrophy can be recapitulated on stimulation of cultured neonatal rat ventricular myocytes (NRVMs) with the paracrine modulator endothelin-1 (ET-1). Multiple signaling pathways are activated by ET-1 stimulation, including MAPK cascades and IP<sub>3</sub>-dependent calcium release.

Application of ET-1 (100 nM) to NRVM for 24 hours increased expression of the hypertrophic marker atrial natriuretic factor (ANF) at both the mRNA and protein level. The MEK1 inhibitor PD184352 (1  $\mu$ M) inhibited the response to ET-1. This effect was observed both in the presence and absence of voltage-gated calcium cycling. ET-1 also increased mRNA levels of dual specificity phosphatase 6 (DUSP6), a negative regulator of the ERK1/2 cascade. Overexpression of DUSP6 by adenoviral infection inhibited both basal and agonist-induced ANF expression. The mechanism underlying ERK1/2-dependent gene expression was investigated by monitoring the activity of an AP-1-dependent luciferase reporter construct. Application of ET-1 increased AP-1 luciferase activity in a PD184352-sensitive manner. To further characterize the significance of ERK1/2 signaling, workload-induced hypertrophy was modeled by enhancing global calcium signals with BayK 8644, an L-type calcium channel agonist. Inhibition of ERK1/2 prevented BayK 8644-induced hypertrophy. Intriguingly, BayK 8644 did not induce AP-1-dependent transcriptional activity.

In summary, these results indicate that ERK1/2 activity is necessary for gene expression induced by multiple hypertrophic agonists. In the absence of global calcium signals, sensitivity to ERK1/2 inhibition persists. This suggests that ERK1/2 activity is necessary for the induction of hypertrophy-associated gene expression under conditions that solely elicit IP<sub>3</sub>-dependent calcium release, which is itself necessary for the hypertrophic response. Although both ET-1 and BayK 8644 induce an ERK1/2-dependent hypertrophic pattern of gene expression, only ET-1 elicits AP-1 transcriptional activity.

This implies that additional transcriptional regulators must be involved in the hypertrophic response.

**26. Calcium and Blood Flow Regulation.** HÉLÈNE GIROUARD,<sup>1</sup> ADRIAN D. BONEV,<sup>1</sup> RACHAEL HANNAH,<sup>1</sup> ANDREA MEREDITH,<sup>2</sup> RICHARD ALDRICH,<sup>3</sup> and MARK T. NELSON,<sup>1</sup> *<sup>1</sup>Department of Pharmacology, University of Vermont, Burlington, VT 05405; <sup>2</sup>Department of Physiology, University of Maryland, Baltimore, MD 21201; <sup>3</sup>Department of Neurobiology, University of Texas, Austin, TX 78712*

Functional hyperemia, a vasodilatory response to increased neuronal activity, ensures an adequate supply of nutrients and oxygen to active brain regions. Increased intracerebral blood flow in response to neuronal activity is a fundamental physiological process that is exploited diagnostically, forming the basis for techniques such as functional magnetic resonance imaging (fMRI), which uses both perfusion and blood oxygenation level-dependent (BOLD) contrast to map brain function.

Recent evidence indicates that neuronal activity is encoded in astrocytes in the form of dynamic intracellular calcium (Ca<sup>2+</sup>) signals, which travel to astrocytic processes ("endfeet") encasing the arterioles in the brain. Astrocytic Ca<sup>2+</sup> signaling has been implicated in the dilatory response of adjacent arterioles, in keeping with the functional linkage between neuronal activity and enhanced local blood flow. Paradoxically, however, astrocytic Ca<sup>2+</sup> signals have also been linked to constriction.

Here, we show that regardless of the mechanism by which astrocytic endfoot Ca<sup>2+</sup> was elevated, modest increases in Ca<sup>2+</sup> induced dilation, whereas larger increases switched dilation to constriction. Large-conductance, Ca<sup>2+</sup>-sensitive potassium (BK) channels in astrocytic endfeet mediate a majority of the dilation and the entire vasoconstriction, implicating local extracellular K<sup>+</sup> as a vasoactive signal for both dilation and constriction. K<sup>+</sup> efflux through astrocytic endfoot BK channels could lead to a rapid dilation or constriction of adjacent arterioles, depending on its local perivascular concentration. Elevation of external K<sup>+</sup> to 20 mM or less activates smooth muscle (SM) inward rectifier potassium channels, causing SM hyperpolarization, closing of SM voltage-dependent calcium channels, a decrease in SM calcium, and thereby vasodilation. Elevation of external K<sup>+</sup> above 20 mM causes SM depolarization and vasoconstriction. These results provide evidence for a unifying mechanism that explains the nature and apparent duality of the vascular response, showing that the degree and polarity of neurovascular coupling depends on extracellular K<sup>+</sup> and astrocytic endfoot Ca<sup>2+</sup>.

**27. The Rapid Actions of Anabolic-Androgenic Steroids (AAS) Are Mediated through the Epidermal Growth Factor Receptor (EGFR).** M.M. HAMDI and G. MUTUNGI, *Biomedical and Clinical Sciences Research Insti-*

tute, School of Medicine, Health Policy and Practice, University of East Anglia, NR4 7TJ Norwich, England, UK

It is now generally believed that anabolic-androgenic steroids (AAS) have both genomic and nongenomic actions (Lösel, R.M., E. Falkenstein, M. Feuring, A. Schultz, H.-C. Tillmann, K. Rossol-Haseroth, and M. Wehling. 2003. *Physiol. Rev.* 83:965–1016). The genomic actions of AAS take several hours to days to be manifested and are mediated through the androgen receptor, a member of the nuclear receptor family (Heinlein, C.A., and C. Chang. 2002. *Mol. Endocrinol.* 16:2181–2187). In contrast, the rapid actions of AAS are evident within minutes and may be effected through second messenger signaling mechanisms initiated by the attachment of these hormones to a G protein-coupled receptor on the cell surface (Estrada, M., A. Espinosa, M. Muller, and E. Jaimovich. 2003. *Endocrinology*. 144:3586–3597). However, the receptor involved remains uncertain. Therefore, the primary aim of this study was to investigate the identity of this receptor.

The experiments were performed using small muscle fiber bundles isolated from either the extensor digitorum longus (a fast-twitch muscle) or soleus (a slow-twitch muscle) of adult female CD-1 mice aged  $49 \pm 5$  days. The fiber bundles were treated with DHT, DHT plus various inhibitors, or the vehicle only. During an experiment, maximum isometric tension ( $P_o$ ) was measured and the fiber bundles were processed for immunoblotting.

Our results show that treating the fiber bundles with DHT increased  $P_o$  in fast-twitch fibers but decreased it in the slow-twitch fibers. It also led to a two- to threefold increase in the phosphorylation of extracellular signal-activated kinases 1/2 and the 20-kD regulatory myosin light chains in both fiber types. Moreover, all these effects could be reversibly blocked by AG1478 but not by flutamide and cyproterone acetate. From these results, we suggest that DHT exerts its rapid actions, in intact mammalian skeletal muscle fibers, through the EGFR.

28. Investigating the Putative Role in Muscle Hypertrophy of the Novel Skeletal Muscle-specific Protein *IGFN1*. ANDREW HAYNES, JANE BAKER, GENNA RILEY, and GONZALO BLANCO, *Mammalian Genetics Unit, MRC Harwell, Science and Innovation Campus, Oxfordshire OX11 0RD, England, UK*

KY is a 72-kD protein that underlies the *ky-kyphoscoliotic* muscular dystrophy in the mouse (Blanco, G., G.R. Coulton, A. Biggin, C. Grainge, J. Moss, M. Barrett, A. Berquin, G. Maréchal, M. Skynner, P. van Mier, et al. 2001. *Hum. Mol. Genet.* 10:9–16). A yeast two-hybrid (Y2H) screen with KY as bait revealed interactions with several sarcomeric proteins, including filamin C and a fragment of a novel protein provisionally named KYIP1 (KY-interacting protein 1) (Beatham, J., R. Romero, S.K. Townsend, T. Hacker, P.F. van der Ven, and G. Blanco. 2004. *Hum. Mol. Genet.* 13:2863–2874), now renamed

IGFN1 (immunoglobulin and fibronectin 3-containing protein 1). Our analysis revealed that *Igfn1* is a complex locus conserved in all available mammalian genomes. Encoded here are IGFN1, a large skeletal muscle-specific protein, and other smaller isoforms showing a wider expression profile. IGFN1 contains two segments spanning three and eight globular domains located at the N and C termini of the protein, respectively, and separated by a large unstructured region lacking any recognizable domain. Y2H, biochemical, and immunofluorescence experiments have provided evidence that IGFN1, KY, and FLNC are members of a protein complex that localize to the sarcomeric Z-band. However, in adult skeletal muscle IGFN1 behaves as a Z-band-associated protein that is also present in the nucleus. Here, we show that the three N-terminal globular domains of IGFN1 are sufficient to provide both nuclear localization and Z-band targeting in transduced cardiomyocytes and transgenic lines. Consistent with those observations, IGFN1 immunohistochemistry of adult muscle shows clear Z-band staining as well as nuclear staining in a proportion of myonuclei. However, atrophic muscles in the *ky/ky* mouse mutant, such as soleus, do not show IGFN1 staining in the nucleus. We hypothesize that the Z-band KY protein complex could be involved in mediating a response to changes in tension or overload, and that IGFN1 could act as a link to the nucleus to influence transcriptional changes. This hypothesis is being tested using mouse transgenic and *in vitro* models.

29. A Mutation Associated with DCM Increases Phospholamban (PLB) Oligomerization and Decreases SERCA Binding, but Does Not Change PLB Tertiary Structure or Phosphorylation by PKA. ZHANJI HOU,<sup>1</sup> RAFFAELLO VERARDI,<sup>2</sup> LARRY R. MASTERSON,<sup>2</sup> NAOMI MENARDS,<sup>2</sup> KIM N. HA,<sup>2</sup> ALESSANDRO MASCIONI,<sup>2</sup> GIANLUIGI VEGLIA,<sup>2</sup> and SETH L. ROBIA,<sup>1</sup>

<sup>1</sup>*Loyola University Chicago, Maywood, IL 60153; <sup>2</sup>University of Minnesota, Minneapolis, MN 55455*

To better understand the pathological mechanism of a human dilated cardiomyopathy phospholamban (PLB) mutation (R9C), we investigated the effects of this mutation on PLB structure and regulatory interactions. Notably, we observed efficient phosphorylation of R9C-PLB by PKA *in vitro*, and nuclear magnetic resonance (NMR) spectroscopy showed no change in R9C-PLB structure compared with WT. However, R9C-PLB reconstituted into lipid vesicles showed increased sensitivity to oxidizing conditions, responding to peroxide challenge with a decreased electrophoretic mobility suggestive of increased oligomerization. This oligomeric species was characterized by a high thermal stability compared with WT pentamers. To test R9C-PLB binding interactions in live cells, PLB was expressed as cyan and yellow fluorescent protein (CFP/YFP) fusions

in AAV-293 cells, and PLB oligomerization and SERCA binding were quantified by fluorescence resonance energy transfer (FRET). 100  $\mu$ M H<sub>2</sub>O<sub>2</sub> applied to the cells induced a rapid quench of CFP-R9C-PLB fluorescence and a concomitant increase in YFP-R9C-PLB fluorescence, indicating an increase in intraoligomeric FRET after oxidation. FRET enhancement after peroxide addition was not observed for CFP/YFP-WT-PLB. To test whether the FRET increase was due to increased oligomerization or a quaternary conformation change, we measured intraoligomeric FRET in a population of cells expressing a wide range of R9C-PLB protein concentrations. FRET dependence on concentration yielded oligomer-intrinsic FRET efficiency (FRET<sub>max</sub>) and relative dissociation constant (K<sub>D</sub>). Compared with WT, R9C-PLB had a decreased K<sub>D</sub> and increased FRET<sub>max</sub>, indicating an increased oligomerization affinity and more compact oligomer structure, respectively. The enhanced oligomerization of R9C-PLB was matched by a decrease in SERCA binding compared with WT. Overall, the data suggest a new mechanism by which the R9C mutation may exert a pathological effect: decreased SERCA regulation and increased oligomerization, as consequences of increased oxidation sensitivity of R9C-PLB.

30. FRET Microscopy Reveals that PLB Binds More Avidly to SERCA1a than SERCA2a. ZHANJI HOU and SETH L. ROBIA, *Department of Physiology, Loyola University Chicago, Maywood, IL 60153*

Phospholamban is expressed at high levels in the heart, where it is the major regulator of the calcium pump SERCA2a. However, it is also present at lower levels in skeletal muscle, where both SERCA1a and SERCA2a variants are present. These SERCA isoforms have been used interchangeably in mutagenic and structural analyses of the PLB-SERCA interaction, since in vitro studies have shown their functional inhibition by PLB is equivalent. To quantify the quaternary structure and binding energetics of PLB binding to SERCA isoforms, Förster resonance energy transfer (FRET) from CFP-SERCA1a or CFP-SERCA2a to YFP-PLB was measured in live AAV-293 cells. FRET efficiency increased with increasing protein expression level to a maximum of 28.8% for PLB-SERCA1a and 28.1% for PLB-SERCA2a, suggesting that the complexes have the same quaternary conformation. Unexpectedly, the data also revealed that PLB has a 2.6-fold higher apparent affinity for SERCA1a relative to SERCA2a. To test whether the observed difference in affinity arises from differential distributions of SERCA E1/E2 enzymatic substates, cells were treated with 1 mM EGTA and 0.5  $\mu$ L/ml calcium ionophore A23187. Under these conditions, PLB still showed greater affinity for SERCA1a over SERCA2a, suggesting that the differential affinities are intrinsic properties of the SERCA isoforms. The data suggest

that PLB preferentially binds SERCA1a over SERCA2a, a selectivity that may be functionally significant in skeletal muscle.

31. Modeling the Intramuscular Signals that Regulate Muscle Protein Degradation. LEWIS A. JACOBSON<sup>1</sup> and NATHANIEL J. SZEWCZYK,<sup>2</sup> <sup>1</sup>*Department of Biological Sciences, University of Pittsburgh, Pittsburgh, PA 15260;*

<sup>2</sup>*University of Nottingham, School of Graduate Entry Medicine and Health, Derby City General Hospital, Derby DE22 3DT, England, UK*

Muscle protein degradation is associated with a variety of human diseases and is thought to be regulated by at least a dozen extra-muscular signals. We have spent several years developing *C. elegans*, a genomic model organism, into a model for studying the intramuscular signals that regulate cytosolic muscle protein degradation. As of April 1, 2009, we have examined 324 genes (of roughly 20,000 total or 3,000 muscle enriched) by mutation and/or RNAi and have found 64 genes that regulate muscle protein synthesis and/or degradation. We have discovered that: (1) proteasome-mediated degradation is negatively regulated by genes that regulate depolarization of the plasma membrane and intra-muscular calcium release; (2) autophagy-mediated degradation is combinatorially regulated by negative signal from insulin and TGF- $\beta$  receptors and positive signal from a constitutive, autocrine FGF signal; (3) apparent calpain-mediated degradation is negatively regulated by a variety of integrin-linked molecules at the costamere; (4) as many as 20% of kinases (100 of 450 have been tested) and 30% of genes that regulate muscle contraction (105 of  $\sim$ 2,000 have been tested) may act to regulate cytosolic muscle protein degradation. In so far as they have yet been examined, identical signals appear to function in mammalian muscle. Although the regulatory network controlling muscle protein degradation in human beings likely involves additional components, connections, and thus complexity, *C. elegans* appears to be a good model for understanding the evolutionarily conserved elements that regulate muscle protein degradation.

<sup>1,2</sup>NIH NIAMS R01AR054342; <sup>1</sup>NSF MCB-0542355; and <sup>2</sup>MRC G0801271.

32. Specific Pattern of Ionic Channel Gene Expression Associated with Proliferation of Vascular Smooth Muscle Cells. JOSÉ RAMÓN LÓPEZ-LÓPEZ,<sup>1</sup> PILAR CIDAD,<sup>1</sup> ALEJANDRO MORENO-DOMÍNGUEZ,<sup>1</sup> LAURA NOVENSÁ,<sup>2</sup> MERCÉ ROQUÉ,<sup>2</sup> MAGDA HERAS,<sup>2</sup> and M. TERESA PÉREZ-GARCÍA,<sup>1</sup> <sup>1</sup>*Departamento de Bioquímica y Biología Molecular y Fisiología e Instituto de Biología y Genética Molecular (IBGM), Universidad de Valladolid y CSIC, 47003 Valladolid, Spain;* <sup>2</sup>*Servicio de Cardiología. Institut Clinic del Tòrax, Hospital Clinic, IDIBAPS, Universidad de Barcelona, 08007 Barcelona, Spain*

Vascular smooth muscle cells (VSMCs) regulate vessel diameter and determine tissue perfusion. However, they also contribute significantly to occlusive vascular diseases by virtue of its ability to switch to an activated, noncontractile, migratory, and proliferating phenotype. Although the participation of ion channels in this phenotypic switch has been previously described, the changes in their expression are poorly defined mainly due to their large molecular diversity. Here, we used high-throughput real-time PCR to obtain a global portrait of ion channel expression in contractile VSMCs from mouse femoral arteries, exploring changes upon phenotypic switch in two experimental paradigms: an *in vivo* model of endoluminal lesion–induced neointimal hyperplasia and an *in vitro* model in which cultured VSMCs were obtained from explants. The channel genes studied included K<sup>+</sup> channels ( $\alpha$ ,  $\beta$ , and  $\gamma$  subunits) and  $\alpha$  subunits of voltage-dependent Ca<sup>2+</sup> channels (VDCC), Cl<sup>-</sup>, and TRP channels. The analysis of changes in mRNA expression of these channels showed a good correlation between the two proliferative models, with 16 genes displaying significant variation in both conditions. Among those, only two genes, Kv1.3 and Kv $\beta$ 2, increased their expression in proliferative VSMCs. By combining immunological and electrophysiological techniques, we explore the expression and the functional contribution of these proteins in contractile and proliferating VSMCs. Our data show that Kv1.3 currents become the predominant outward K<sup>+</sup> current in cultured VSMCs. Moreover, we found that the up-regulation of Kv1.3 currents in these cells is an essential component of the phenotypic switch, as the specific blockade of Kv1.3 channels inhibits VSMCs migration and proliferation. Collectively, our results pinpoint Kv1.3 channels as new therapeutical targets for the treatment of vascular disorders involving VSMC proliferation.

Supported by Heracles network (grant R006/009), Spanish Department of Science (grant BFU2007-61524), and Junta de Castilla y León (grant GR242).

33. The TRPP Channel PKD1L2 Is Linked with a Complex Neuromuscular Disease in the Mouse. FRANCESCA E. MACKENZIE, ROSARIO ROMERO, DEBBIE WILLIAMS, HELEN HILTON, TERTIUS HOUGH, LINDA GREENSMITH, RICHARD R. RIBCHESTER, and GONZALO BLANCO, *MRC Mammalian Genetics Unit, Harwell OX11 0RD, England, UK*

*Ostes* is a novel *N*-ethyl *N*-nitrosourea (ENU)-induced mouse mutant with muscle atrophy. *Ostes* mice suffer chronic neuromuscular impairments, including neuromuscular junction degeneration, polyneuronal innervation, and myopathy. Analysis of 23 other tissues, including heart, did not reveal any other pathological change. Genetic mapping identified a small region on distal chromosome 8 segregating with the *Ostes* phenotype. Sequence analysis of that chromosomal segment

revealed no coding or splicing mutation in any of the annotated genes. However, expression studies indicated accumulation of the protein PKD1L2 in skeletal muscle from *ostes/ostes* mice. Because the mutation provoking up-regulation of the linked gene *Pkd1l2* has not yet been identified, we tested the hypothesis that overexpression of this gene is causative by generating a transgenic line with a BAC clone spanning *Pkd1l2* and one flanking gene on each side. The flanking genes, *Gcsh* and *Bcmol*, were ruled out as candidates for this disease, as their expression was normal in *ostes/ostes* mice and their exons and cDNAs contained no mutation. Transgenic mice *Tg(Pkd1l2)/Tg(Pkd1l2)* reproduced the *ostes* myopathic changes, including fiber size asymmetry, small but significant reduction of the cross-sectional area of type II fibers, regeneration, and lack of macrophage infiltration. Muscle atrophy in *Tg(Pkd1l2)/Tg(Pkd1l2)* mice was more severe than in *ostes/ostes* mice. Moreover, double heterozygous mice (*ostes/+*, *Tg(Pkd1l2)/0*) suffer myopathic changes more profound than each heterozygote, indicating positive correlation between PKD1L2 levels and disease severity. We show that, *in vivo*, PKD1L2 primarily associates with endogenous fatty acid synthase (FASN) in normal skeletal muscle, and these proteins appear to colocalize to costameric regions of the muscle fiber. In diseased *ostes/ostes* muscle, both proteins are up-regulated and *ostes/ostes* mice show signs of abnormal lipid metabolism. In conclusion, our data suggest that PKD1L2 up-regulation is a cause of neuromuscular defects in mice.

34. A New Molecular Mechanism for Familial Dilated Cardiomyopathy Based on Studies with Intact Mutant Transgenic Mouse and Human Explanted Heart Muscle. STEVEN B. MARSTON, EMMA C. DYER, ADAM M. JACQUES, ANDREW E. MESSER, DOMINIC WELLS, and WEIHUA SONG, *Imperial College London, London SW7 2AZ, England, UK*

Familial dilated cardiomyopathy (DCM) can be caused by mutations in sarcomeric proteins. Studies of DCM mutations in TnT, TnC, and tropomyosin in recombinant protein *in vitro* indicated a common molecular phenotype with reduced Ca<sup>2+</sup> sensitivity and cross-bridge cycling rate. However, investigations in more organized systems contradict this mechanism, putting its physiological relevance in doubt.

We investigated native thin filament Ca<sup>2+</sup>-regulatory properties using actin from a transgenic mouse expressing the E361G DCM-causing mutation combined with human cardiac troponin and tropomyosin.

In *in vitro* motility assays (IVMAs) we could observe no differences between E361G and NTG mouse thin filaments; however, when troponin was dephosphorylated with acid phosphatase, we observed that E361 Ca<sup>2+</sup> sensitivity was lower than NTG, as previously found with the recombinant proteins (ratio of EC<sub>50</sub> 1:2.6). When we

compared natively phosphorylated and dephosphorylated thin filaments, we observed that  $\text{Ca}^{2+}$  sensitivity did not change in E361G mouse thin filaments, but the  $\text{Ca}^{2+}$  sensitivity increased 3.1 times on dephosphorylation of NTG mouse as expected. Thus, the only functional change induced by the E361G mutation in cardiac actin was a blunted response to troponin I phosphorylation. This would be predicted to compromise the lusitropic response to catecholamines.

In addition, we studied troponin extracted from the explanted heart of a DCM patient carrying the cardiac TnC G159D mutation. IVMA investigation of reconstituted thin filaments showed that the cTnC G159D mutation also showed little change in  $\text{Ca}^{2+}$  sensitivity when TnI was dephosphorylated ( $\text{EC}_{50} \text{ P/unP} = 1.2 \pm 0.2$ ). TnC G159D troponin also showed a higher  $\text{Ca}^{2+}$  sensitivity than donor heart troponin, regardless of phosphorylation status.

We propose that the DCM phenotype is caused by uncoupling of the relationship between phosphorylation and  $\text{Ca}^{2+}$  sensitivity.  $\text{Ca}^{2+}$  sensitivity is not correlated with DCM, but the phosphorylation status of troponin I and other posttranslational modifications of sarcomeric proteins are critical determinants of the functional effects of a mutation.

**35. Pump Dysfunction and Depressed Contractile Reserve in a Murine Model of Hypertrophic Cardiomyopathy.** **RICHARD L. MOSS** and **CARL TONG**, *Department of Physiology, University of Wisconsin School of Medicine and Public Health, Madison, WI 53705*

Heritable hypertrophic cardiomyopathies (HCMs) are the most common cause of unexpected sudden death in the young and are due in most cases to a point mutation in one of several sarcomeric proteins, including  $\beta$  myosin heavy chain, myosin binding protein C, and regulatory proteins associated with the thin filament. HCMs are characterized by accelerated contraction during systole, but cardiac function is paradoxically reduced. To study the basis for these phenomena, we have developed a murine model of hypertrophic cardiomyopathy due to disruption of the *MYBPC3* gene that encodes cardiac myosin binding protein C (cMyBP-C), a thick filament accessory protein that is thought to have both structural and regulatory roles in striated muscle contraction. This disruption of the gene results in ablation of cMyBP-C, which is similar to the molecular phenotype observed in human patients with HCM due to C-terminal truncations of cMyBP-C in which sarcomeric cMyBP-C content is reduced. Hearts from these mice exhibit septal hypertrophy, increased chamber size, and reductions in both stroke volume and the period of ejection. Myocardium from these mice exhibit depressed twitch force-frequency relationships, accelerated relaxation kinetics, and a loss of both frequency-dependent and  $\beta$  agonist-induced acceleration of relaxation. These results can be

explained by an acceleration of cross-bridge interaction kinetics due to the ablation of cMyBP-C, which in turn cause an acceleration of twitch kinetics, a reduction in peak force or pressure, and reduced stroke volume.

**36. Cardiomyocytes from Human Embryonic Stem Cells.** **CHRISTINE MUMMERY**, *Department of Anatomy and Embryology, Leiden University Medical Centre, 2300 RC Leiden, Netherlands*

#### Stem cells and development

Derivation of heart cells from human embryonic stem cells (HESCs) and understanding the underlying developmental mechanisms is the main focus of the research. Culture conditions have now been sufficiently refined so that cardiomyocyte differentiation is an efficient and reproducible process. Microarray analysis of modulations in gene expression during differentiation has shown that the major known cardiac genes are upregulated but that novel genes are also expressed.

Genetically marked HESCs have been produced in which expression of the green fluorescent protein marker is retained after differentiation. This has permitted unambiguous tracing of cardiomyocytes after transplantation into a mouse heart. Long-term survival of the cells and integration into the host heart have been observed, and the ability of these cells to restore cardiac function in mice that have undergone myocardial infarction is being investigated. More immediate applications of HESC-derived cardiomyocytes are being sought in drug discovery and disease.

**37. Exploring the Role of IGFN1 Variants in Cardiac Muscle.** **GENNA RILEY, JANE BAKER, ROSARIO ROMERO, HELEN HILTON, and GONZALO BLANCO**, *Mammalian Genetics Unit, MRC Harwell, Oxfordshire OX11 0RD, England, UK*

A fragment of the novel protein, IGFN1, was identified as an interacting partner of the sarcomeric protein, KY, the loss of which underlies a form of postural muscle-specific muscular dystrophy in the mouse (*kyphoscoliotic* mutant). IGFN1 has a predicted domain composition comparable to that of other sarcomeric support proteins, including filamin C, myosin binding protein C, and titin. Disruption within these genes is recognized as being associated with muscular dystrophies and cardiomyopathies. Hence, it was postulated that IGFN1 may also contribute to the degenerative molecular pathways common to these striated muscle-specific diseases.

In this work, northern analysis revealed that GENSCAN predicted *Igfn1*, which is not expressed in the heart but is exclusively expressed in skeletal muscle, with smaller isoforms expressed in both tissues. These findings are substantiated by Western blot analysis using isoform-specific antibodies. Several proteins have

been identified in heart extracts as putative IGFN1 products with molecular weights of 189, 135, and 64 kD, with the 135-kD isoform being the most predominantly expressed form. Immunofluorescent analysis of heart cryosections and primary cultured murine cardiomyocytes using antibodies raised against the C terminus of IGFN1 produced prominent intercalated disk staining. Ultrastructural analysis refined this localization to the adherens junction. Furthermore, peptide mass finger-print analysis and liquid chromatography followed by tandem mass spectroscopy of IGFN1-immunoprecipitated complexes identified N-cadherin,  $\beta$ -catenin, and plakoglobin, three well-characterized proteins of the adherens junction, as interacting partners of the 135-kD IGFN1 variant. Collectively, this work tentatively suggests that cardiac IGFN1 is a newly identified structural component of this specialized junction. To validate these results, cloning and expression of the major heart-specific isoform in primary cardiomyocytes are currently being undertaken.

38. Mouse HCM Model Expression E99K ACTC Mutation Reproduces the Clinical HCM Phenotype. WEIHUA SONG,<sup>1</sup> DANIEL J. STUCKEY,<sup>2</sup> EMMA DYER,<sup>1</sup> DOMINIC WELLS,<sup>1</sup> SIAN E. HARDING,<sup>1</sup> CAROLYN A. CARR,<sup>2</sup> KIERAN CLARKE,<sup>2</sup> and STEVEN B. MARSTON,<sup>1</sup> <sup>1</sup>*Imperial College London, London SW7 2AZ, England, UK;* <sup>2</sup>*Oxford University, Oxford OX1 2JD, England, UK*

The mutation Gly99lys (E99K) in the cardiac actin (ACTC) gene causes hypertrophic cardiomyopathy (HCM). Transgenic (TG) mice expressing 50% E99K mutant cardiac actin in their hearts were generated and studied. Over 30% male and 70% female E99K mice died between 28 and 45 days just after adolescence.

We studied mutant actin from the survivors by in vitro motility assay. Thin filaments were reconstituted with purified mouse f-actin and human heart tropomyosin and troponin. The E99K thin filaments were  $2.5 \pm 0.6$  times more  $\text{Ca}^{2+}$  sensitive than NTG thin filaments ( $P = 0.05$ ). E99K actin thin filaments also exhibited a reduced response to troponin dephosphorylation.

Isofluorane-anesthetized 7 month-old male TG mice ( $n = 9$ ) and their NTG littermates ( $n = 7$ ) were studied using in vivo cine MRI. Abnormal cardiac morphology and significantly lower ejection fractions ( $P = 0.01$ ) and reduced stroke volumes ( $P < 0.001$ ) were observed in the TG mice. Peak LV ejection rates were reduced ( $P = 0.01$ ).

Left ventricle function of 9 month-old female NTG ( $n = 4$ ) and TG ( $n = 5$ ) mice were studied with an in vivo conductance catheter through apex after an anterior thoracotomy under isoflurane. The TG mice had significantly reduced ejection fraction ( $P = 0.01$ ), increased end-diastolic pressure ( $P = 0.02$ ), and impaired relaxation ( $\text{Tau}_g, P = 0.003$ ). LV dilation has been observed

in these mice (end-systolic volume,  $P < 0.0001$ ; end diastolic volume,  $P = 0.04$ ).

The ACTC E99K mouse reproduces many features of HCM as observed in patients: sudden death, partial penentrance, impaired relaxation, asymmetrical and apical hypertrophy, and progression toward a dilated failing heart. The basic effect of the ACTC E99K mutation is increased  $\text{Ca}^{2+}$  sensitivity together with a blunted response to troponin I phosphorylation.

The increased myofibrillar  $\text{Ca}^{2+}$  sensitivity may be sufficient to provoke arrhythmia in E99K mice and account for the high mortality at early ages. Hypertrophy may be a chronic response to  $\text{Ca}^{2+}$  overloading or be due to energy depletion.

39. Role of the Calcineurin (CnA)/NFAT Pathway in Pathological and Physiological Forms of Cardiac Myocyte Hypertrophy. AMARNATH TALASILA,<sup>1</sup> MARTIN D. BOOTMAN,<sup>1</sup> and H. LLEWELYN RODERICK,<sup>1,2</sup>

<sup>1</sup>*Laboratory of Molecular Signaling, Babraham Institute, Cambridge CB22 3AT, England, UK;* <sup>2</sup>*Department of Pharmacology, University of Cambridge, Cambridge CB2 1PD, England, UK*

We have recently shown that induction of pathological cardiac hypertrophy by endothelin-1 (ET-1) is dependent on activation of the CnA/NFAT pathway by  $\text{InsP}_3$ -induced  $\text{Ca}^{2+}$  release (IICR) in the nucleus. Although the requirement of the CnA/NFAT pathway in pathological hypertrophy is established, whether it has a role in physiological hypertrophy is debated. Here, we tested the hypothesis that IICR-mediated activation of the CnA/NFAT pathway acts as a molecular switch to determine the nature of the hypertrophic response (physiological vs. pathological).

Experiments were performed in neonatal rat ventricular myocytes. Insulin-like growth factor-1 (IGF-1) was used to stimulate physiological hypertrophy and ET-1 to induce pathological hypertrophy. Hypertrophy was assessed by real-time PCR analysis of mRNA levels of the hypertrophy markers atrial natriuretic factor (ANF), brain natriuretic peptide (BNP), and  $\alpha$ -skeletal actin ( $\alpha$ -SKA), and by measuring protein synthesis by [<sup>3</sup>H]-leucine incorporation.

IGF-1 significantly increased the mRNA level of  $\alpha$ -SKA and protein synthesis, but unlike ET-1, it did not induce ANF and BNP. In these beating myocytes, inhibition of CnA activity with cyclosporin A prevented the action of IGF without affecting that of ET-1. The activity of an NFAT luciferase reporter (NFAT-luc) was significantly increased by both ET-1 and IGF-1. Inhibition of IICR by expression of  $\text{InsP}_3$  5'-phosphatase abolished the activation of the NFAT-luc by both hypertrophic mediators. Under conditions where excitation-contraction coupling (ECC)-associated  $\text{Ca}^{2+}$  transients were blocked with nifedipine and mibepradil, NFAT-luc activity was sensitive only to  $\text{InsP}_3$  5'-phosphatase upon ET-1

stimulation. In ECC-blocked cells, both ET-1 and IGF-1 caused an increase in protein synthesis, but only after ET-1 stimulation was IICR dependent.

These data show that the CnA/NFAT pathway is activated by IICR after stimulation with the inducers of both physiological and pathological hypertrophy. Our data may also suggest that a background of global ECC-associated  $\text{Ca}^{2+}$  signals is required for the induction of physiological hypertrophy by IICR-mediated activation of NFAT.

40. Myostatin Inhibits Calcium-dependent Signaling Pathways Activated by IGF-1 in Myoblast. JUAN ANTONIO VALDÉS and ALFREDO MOLINA, *Facultad de Ecología y Recursos naturales, Universidad Andrés Bello, Santiago, Chile*

The myogenic program involves several coordinated steps (myoblast proliferation, differentiation, and fusion) regulated by extracellular cues, like myostatin and insulin-like growth factor-1 (IGF-1). IGF-1 is a positive regulator in proliferation and differentiation of skeletal muscle cells, whereas myostatin acts as a negative regulator of skeletal muscle mass. Both growth factors have potential application in the biomedical field. IGF-1 expression in muscle ameliorates tissue deterioration caused by diverse myopathies; meanwhile, the inhibition of myostatin signaling pathways holds great promise for the treatment of muscle-wasting diseases.

These growth factors exert their antagonist functions, activating different transduction pathways mediated by their receptors. Myostatin has been shown to bind to activin type II receptors (serine/threonine kinase receptor family), activating a signal transduction pathway that leads phosphorylation of the transcriptions factors Smad2/Smad3, which ultimately leads to suppression of myogenesis. On the other hand, almost all biological actions of IGF-1 are mediated by binding to the IGF-1 receptor (tyrosine kinase receptor family), activating transduction pathways mediated by phosphoinositide 3-kinase (PI3K) related to muscle proliferation, differentiation, protein synthesis, and hypertrophy.

However, recently experimental data obtained by our group and others strongly suggest a negative feedback through a cross talk between IGF-1 and myostatin signaling pathways during myogenesis. Using myoblast of skeletal muscle primary culture, we found that IGF-1 induces myostatin mRNA expression through the activation of signaling pathways PI3K and calcineurin dependent, probably mediated by the transcription factor NFAT. In addition, myostatin inhibits calcium release induced by IGF-1 in myoblast and the activation of the transduction pathways PI3K-PLC- IP3-calcineurin-NFAT. Considering these findings, we propose that during myoblast differentiation, IGF-1 regulates myostatin gene expression and, in contrast, myostatin inhibits the IGF-1 signaling pathways. The information obtained in

this project will contribute to the knowledge in the field of muscle development and will help us to understand unexplored areas in signal transduction with potential applications in biomedicine.

41. Spatial Control of  $\text{pH}_i$  in the Heart, and Its Influence on the Local Control of Intracellular  $\text{Ca}^{2+}$  Signaling. RICHARD D. VAUGHAN-JONES,<sup>1</sup> PAWEŁ SWIETACH,<sup>1</sup> and KENNETH W. SPITZER,<sup>2</sup> <sup>1</sup>*Burdon Sanderson Cardiac Science Centre, Oxford OX1 3PT, England, UK;* <sup>2</sup>*Nora Eccles Harrison Cardiovascular Research and Training Institute (CVRTI), Salt Lake City, UT 84112*

$\text{H}^+$  ions and  $\text{CO}_2$  are metabolic end products that must be removed from respiring cells if intracellular pH is to be maintained at its normal value of 7.2. In the heart,  $\text{CO}_2$  is vented diffusively across a myocyte's sarcolemma to the nearest capillary. In contrast,  $\text{H}^+$  ions are extruded on specific ion transporters such as  $\text{Na}/\text{H}$  exchange (NHE1), or neutralized by  $\text{HCO}_3^-$  ions imported on sarcolemmal  $\text{Na}-\text{HCO}_3$  cotransport (NBC). Any spatial non-uniformity of  $\text{pH}_i$  is minimized by high-capacity cytoplasmic shuttling of  $\text{H}^+$  ions on histidyl dipeptides such as carnosine and homocarnosine, which, because they are mobile buffers, can diffusively disperse  $\text{H}^+$  ions. Intracellular  $\text{H}^+$  dispersion also occurs, but to a lesser extent, on the  $\text{CO}_2/\text{HCO}_3$  buffer system. These intracellular shuttles extend between adjacent myocytes, through connexin channels at gap junctions. The channels appear to be both activated and inactivated by  $\text{H}^+$  ions so that, depending on the severity of a local acidosis, they are either opened or closed to  $\text{H}^+$  ion shuttling. Gap junctions therefore provide a local pH-gated control system for the spatial regulation of  $\text{pH}_i$  in the myocardium. Spatial control of  $\text{pH}_i$  may also be provided by exofacial carbonic anhydrase enzymes (CAs), which can facilitate  $\text{CO}_2$  venting from cells, thereby reducing the tendency of aerobic respiration to reduce  $\text{pH}_i$ . The mechanism of spatial  $\text{pH}_i$  regulation by connexins and CAs will be explored in the lecture. The effect of local  $\text{pH}_i$  regulation on the spatial control of systolic and diastolic  $\text{Ca}^{2+}_i$  will also be assessed. It appears that, in ventricular myocytes, intracellular organelles and sarcolemmal  $\text{pH}_i$  regulatory transporters are intimately involved in the local control of  $\text{Ca}^{2+}$  signaling. Intracellular pH is thus a major spatial controller of  $\text{Ca}^{2+}_i$  in the heart. Such spatial control of  $\text{Ca}^{2+}_i$  will thus be disrupted during events such as regional myocardial ischaemia, which is associated with a failure of the local  $\text{pH}_i$  control system.

42. The Physiology and Pathophysiology of Uterine Smooth Muscle. SUSAN WRAY, SARAH ARROWSMITH, KAREN NOBLE, AMANDA HEATH, SIOBHAN QUENBY, and THEODOR BURDYGA, *Physiology Department, Biomedical Sciences, University of Liverpool, Liverpool L69 3BX, England, UK*

The control of uterine muscular activity is clearly necessary for successful reproduction. Our understanding of how these contractions arise and the role of intracellular Ca signals has increased greatly in the last decade. Despite this, preterm labors are still a common problem of childbirth, as are term labors characterized by inadequate uterine contractions. We have sought to obtain a better understanding of how Ca signals spread between cells and muscle bundles in intact myometrium by using confocal imaging, so that a more detailed explanation of how the Ca signal relates to force can be obtained. Our results show that the Ca transients in pregnant uterine tissue are composed of Ca spikes, which are associated with spike-like action potentials. There is large variation in the pattern of spontaneous activity in myometrium, ranging from non-propagating Ca spikes confined to individual smooth muscle cells, through to regional and global propagating Ca spikes. The Ca spikes did not show fixed initiation sites, propagated in longitudinal and transverse directions from the initiation regions, and had a variable pattern of propagation in preparations that were not synchronously active. In preparations that showed synchronous activity, Ca spikes singularly or bursts propagated mainly in the transverse direction from the initiation regions. The amplitude of force generated by single spikes was dependent on the number of bundles recruited by the propagating Ca spike within the strip, and was ~30–40% of the maximal force produced by carbachol or high-K stimulation. If Ca spikes appeared in the form of bursts, they generated longer lasting fused contractions, the amplitudes of which were dependent on the number and the frequency of Ca spikes in the burst.

We have also studied human myometrium from women who have Caesarean sections and characterized uterine activity and Ca signaling associated with diabetes, dysfunctional labors, obesity, fetal distress, and post-term pregnancies. The information from these different patient groups will be discussed and an attempt made to relate it to uterine pathophysiology.

43. A Novel Role for Ryanodine Receptors during Embryonic Development: Studies in Zebrafish. HOUDINI HO-TIN WU, CAROLINE BRENNAN, and RACHEL ASHWORTH, *School of Biological and Chemical Sciences, Queen Mary University of London, London E1 4NS, England, UK*

Embryonic development requires the coordination of complex intracellular signals. Calcium ions ( $\text{Ca}^{2+}$ ) play a variety of roles throughout early embryogenesis; however, the regulation of this messenger in this process is not well established. Ryanodine receptors (RyRs) are a family of intracellular ion channels that control calcium release into the cytosol. We have identified five RyR zebrafish genes (*ryr1a*, *1b*, *2a*, *2b*, and *3*) in zebrafish. Phylogenetic analysis revealed that *ryr1a*, *ryr1b*, and a single *ryr3* gene in zebrafish cluster with those from other teleost species. Zebrafish *ryr2a* was found to be closely related to mammalian homologues, whereas *ryr2b* is more divergent. Semiquantitative end-point PCR and whole mount *in situ* hybridization were used to determine the temporal and spatial expression of RyR mRNA during key stages of development. Maternal expression of *ryr2a*, *2b*, and *3* was detected during the cleavage and blastula periods of zebrafish development; however, the functional significance of this observation remains unclear, as RyRs have not been implicated in very early development. In the somites, *ryr1a* expression was detected in the slow muscle precursors before *ryr1b* expression in the fast fiber progenitor cells, whereas *ryr3* was expressed later throughout the muscle. Expression of *ryr2b* was observed in the precardiac mesoderm from 14 hpf, confirming that this is the cardiac *ryr* gene in zebrafish. The appearance of a heartbeat from 24 hpf onwards confirms the presence of a functional RyR in cardiac muscle, and protein expression was observed at 48 hpf. Finally, the *ryr2a* gene expression could be detected at several sites in the developing forebrain, midbrain, and hindbrain at 24 hpf. The spatial and temporal characterization of *ryr* gene expression will facilitate research into the function of this family of intracellular ion channels during embryogenesis.

## INDEX TO AUTHORS OF ABSTRACTS

*Abstract number follows name*

Aldrich, R., 26  
 Allen, D.G., 21  
 Allen, P.D., 13  
 Angueyra, J.M., 23  
 Arrowsmith, S., 42  
 Ashworth, R., 11, 43  
 Baker, J., 28, 37  
 Bakran, A., 15  
 Bannister, R.A., 13  
 Beam, K.G., 13  
 Bershitsky, B.Y., 3  
 Bezold, K.L., 8  
 Blanco, G., 28, 33, 37  
 Bonev, A.D., 26  
 Bootman, M.D., 39  
 Brault, J.J., 6  
 Brennan, C., 43  
 Burdya, T., 15, 42  
 Camerino, G., 24  
 Carr, C.A., 38  
 Cidad, P., 32  
 Cippone, V., 24  
 Clarke, K., 38  
 Cohen, S., 6  
 Cole, W.C., 20  
 Conte Camerino, D., 24  
 Del Pilar Gomez, M., 22, 23  
 Desaphy, J.-F., 24  
 Digennaro, C., 24  
 Drawnel, F.M., 25  
 Dyer, E.C., 34, 38  
 Eisner, D., 14  
 Eltit, J.M., 13  
 El-Yazbi, A.F., 20  
 Ervasti, J., 2  
 Estève, E., 13  
 Floyd, R.V., 15  
 Franzini-Armstrong, C., 16  
 Gartner, C., 6  
 Gervasio, O.L., 21  
 Giannuzzi, V., 24  
 Girouard, H., 26  
 Glass, D.J., 6  
 Goldberg, A.L., 6  
 Gordienko, D., 17  
 Graham, H.K., 7  
 Greensmith, L., 33  
 Gygi, S.P., 6  
 Ha, K.N., 29  
 Hamdi, M.M., 27  
 Hannah, R., 26  
 Harding, S.E., 38  
 Harhun, M., 17  
 Harris, S.P., 8  
 Haynes, A., 28  
 Heath, A., 42  
 Henderson, D., 2  
 Heras, M., 32  
 Heuser, J., 9  
 Hilton, H., 33, 37  
 Hou, Z., 29, 30  
 Hough, T., 33  
 Huxley, H.E., 10  
 Irving, T., 10  
 Jacobson, L.A., 31  
 Jacques, A.M., 34  
 Johnson, R.P., 20  
 Kashimura, T., 14  
 Katsnelson, L., 19  
 Kim, S., 18  
 Konovalov, P., 19  
 Kopylova, G.V., 3  
 Krivcevska, C., 11  
 Lahne, M., 11  
 Latres, E., 6  
 Liantonio, A., 24  
 Lin, A.Y., 2  
 Lisin, R., 1  
 Liu, K., 13  
 Lookin, O., 1  
 López, J., 13  
 López-López, J.R., 32  
 Loultcheva, L., 9  
 Mackenzie, F.E., 33  
 Markhasin, V.S., 19  
 Marston, S.B., 34, 38  
 Mascioni, A., 29  
 Masterson, L.R., 29  
 Menards, N., 29  
 Meredith, A., 26  
 Messer, A.E., 34  
 Molina, A., 40  
 Moreno-Domínguez, A., 32  
 Moss, R.L., 35  
 Mummery, C., 36  
 Mutungi, G., 27  
 Nasi, E., 22, 23  
 Nelson, M.T., 26  
 Nikitina, L.V., 3  
 Noble, K., 42  
 Novensá, L., 32  
 Pérez-García, M.T., 32  
 Pessah, I.N., 13  
 Pierno, S., 24  
 Povstyan, O., 17  
 Prochniewicz, E., 2  
 Protsenko, Y.L., 1  
 Quenby, S., 42  
 Reconditi, M., 10  
 Rhim, H., 18  
 Ribchester, R.R., 33  
 Riley, G., 28, 37  
 Robia, S.L., 29, 30  
 Roderick, H.L., 25, 39  
 Romero, R., 33, 37  
 Roqué, M., 32  
 Roth, R., 9  
 Schaffer, J.F., 8  
 Shchepkin, D.V., 3  
 Sherratt, M.J., 7  
 Simonetti, S., 24  
 Solaro, R.J., 12  
 Solovyova, O., 19  
 Song, W., 34, 38  
 Spitzer, K.W., 41  
 Stuckey, D.J., 38  
 Sweeney, H.L., 4  
 Swietach, P., 41  
 Szewczyk, N.J., 31  
 Takeya, K., 20  
 Talasila, A., 39  
 Tenkova, T., 9  
 Thomas, D.D., 2  
 Tong, C., 35  
 Trafford, A.W., 7, 14  
 Valdés, J.A., 40  
 Valenzuela, D.M., 6  
 Vaughan-Jones, R.D., 41  
 Veglia, G., 29  
 Venetucci, L., 14  
 Verardi, R., 29  
 Walsh, E.J., 20  
 Walsh, M.P., 20  
 Warshaw, D.M., 5  
 Wells, D., 34, 38  
 Whitehead, N.P., 21  
 Williams, D., 33  
 Winstanley, C., 15  
 Wray, S., 15, 42  
 Wu, H.H.-T., 43  
 Yeung, E.W., 21